IOP Conference Series: Materials Science and Engineering

PAPER • **OPEN ACCESS**

Numerical Investigation of Rough Micro- and Mini-channel Heat Sinks for Varying Aspect ratio

To cite this article: Munib Qasim Ansari and Guobing Zhou 2020 *IOP Conf. Ser.: Mater. Sci. Eng.* **717** 012022

IOP Conf. Series: Materials Science and Engineering **717** (2020) 012022 doi:10.1088/1757-899X/717/1/012022

Numerical Investigation of Rough Micro- and Mini-channel Heat Sinks for Varying Aspect ratio

Munib Qasim Ansari *, Guobing Zhou

School of Energy, Power, and Mechanical Engineering, North China Electric Power University, Beijing 102206, PR China

*E-mail address: munibqasim@icloud.com

Abstract. Numerical simulations are performed to study the impact of aspect ratio on the micro- and mini-channel heat sink behaviours in the presence of sinusoidal surface roughness. A CFD model is first validated with the relevant reference data for laminar flow conditions using ANSYS-Fluent analysis. The found results of this validation study show that the simulation results agree well with the reference data. The considered channel height, absolute roughness height and diameter are 250 µm, 30 µm and 366 to 374 µm, respectively. The top and bottom rough walls are under constant heat flux conditions, while other walls are adiabatic with air as the working fluid. The micro- and mini-channels with long wetted perimeter and lower aspect ratio have shown more convective heat transfer but with slightly higher frictional resistance. The convective heat transfer and thermal performance factor both improve with the increase in Reynolds number where all the values are higher than 1. The maximum value of the thermal performance factor is noted up to 1.6 for the channel having aspect ratio of 0.038 (Reynolds number = 250). This study shows that micro- and mini-channel heat sinks are sensitive to surface roughness, Reynolds number where varying aspect ratio have influence on both flow and heat transfer performances in laminar regime.

1. Introduction

The heat dissipation of electronic devices has become an important factor constraining the rapid development of them. Nowadays, electronic devices tend to be highly integrated within a smaller volume. In this regard, a lot of work has been done to improve the performance of heat sinks without compromising the compactness [1]. Qu and Mudawar [2], and Xi et al. [3] investigated micro- and mini-channels extensively by performing different experiments. In most of these studies, several discrepancies have been reported between the macro-scale correlations and micro-scale flows [4]. The different ways were also applied to enhance the heat transfer performance of micro-channel heat sinks by varying channel shapes [5], heating methods [6] and surface roughness [7].

The configuration of surface roughness can increase the heat transfer performance but at the expense of high-pressure drops. According to Kharati-Koopaee and Zare [8], structured surface roughness is recommended for numerical modeling instead of random surface roughness due to the simplicity of modeling and more detail insight into the flows. Zhang et al. [9] numerically studied the effects of 2D surface roughness and reported that semi-circular shaped roughness could give better performance with fewer flow circulations. Dharaiya et al. [7] also numerically investigated the effects of sinusoidal roughness and found that the maximum heat transfer performance with the maximum deviation from smooth channels was 6.33. Ghani et al. [10] studied the effects of ribs on micro-channels and reported that the maximum performance factor of 1.85 (relative cavity amplitude = 0.15, relative rib width = 0.3 and relative rib length = 0.5, and Reynolds number = 800). Guo et al. [11] also numerically studied the effect of surface roughness and concluded that 3D models are more accurate.

There is not sufficient literature for air as working fluid [8]. Therefore, in this work, micro- and mini-channels are structured with sinusoidal surface roughness and investigated numerically with varying channel width and air as working fluid.

2. Channel and roughness configurations

A single rectangular micro- and mini-channel heat sink is considered for simulation. The top and bottom walls of the channel are devised with sinusoidal surface roughness, as shown in Fig. 1. The width, height, and length of the channel are represented as '*W*',' *H*', and '*L*,' respectively. The working fluid-air flows along the channel length (*x*-axis). Considering the coordinate system shown in Fig. 1, the bottom and top walls are obtained by Eqs. (1) and (2), respectively [8]. Fig. 1(b) elaborates further details where surface roughness pitch, height, and constricted channel height are represented by *s*, *r*, and H_c, respectively.

$$y\,(x) = r cos^4(\frac{\pi}{s}x) \quad \text{Bottom wall} \quad (1) \qquad y\,(x) = H - r sin^4(\frac{\pi}{s}x) \quad \text{Top wall} \quad (2)$$

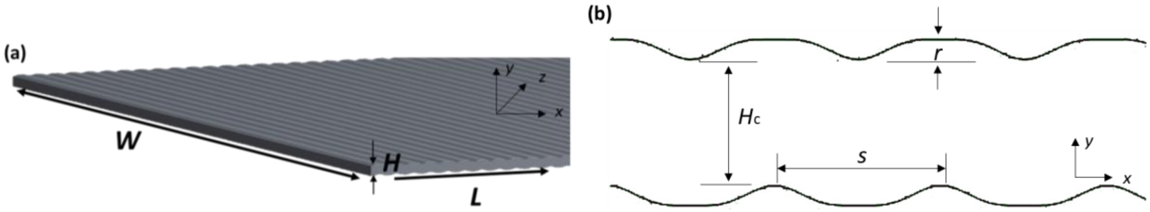

Fig. 1. Schematic of rough micro- and mini-channel heat sink: (a) Stereogram; (b) Front view.

The constricted flow parameter scheme defined by kandlikar et al. [7] is considered for modeling. The corresponding constricted channel height (H_c), hydraulic diameter (D_c) and aspect ratio (α_c) are defined as,

$$H_c = H - 2r \quad (3) \qquad D_c = \frac{4H_cW}{2(H_c+W)} \quad (4) \qquad \alpha_c = {}^{H_c}/_{W} \quad (5)$$

The channel length, channel height, surface roughness height, and pitch are considered as 12.5 mm, 250 µm, 30 µm, and 250 µm, respectively, for all the cases. The aspect ratio variations are based on channel widths (*W*) of 12.7 mm, 8.95 mm and 5 mm, and respective values of constricted aspect ratios (α_c) are 0.015, 0.021 and 0.038.

3. Numerical method

3.1. Governing equations and assessment parameters

The simulated flow is 3D, steady, and assumed incompressible with constant properties. The radiation and gravitational force are neglected in this work. The heated walls are under constant heat flux, while thermo-physical properties are assumed to be constant. The assumptions of no-slip boundary condition, the flow continuum, and Navier-Stokes equation are reasonable in laminar flow regime of the study. The governing equations of continuity, momentum, and energy are written based on the above assumptions:

Continuity equation: $\nabla\vec{V} = 0$ (6)

Momentum equation: $\rho(\vec{V}.\nabla\vec{V}) = -\nabla P + \nabla.(\mu\nabla\vec{V})$ (7)

Energy equation: $\rho C_P(\vec{V}.\nabla T_f) = k_f\,\nabla^2 T_f$ (8)

where P, c_p, μ, T_f, and k_f are fluid pressure, specific heat, dynamic viscosity, fluid temperature, and thermal conductivity, respectively.

For the simulations results, constricted Reynolds number (Re_c), Fanning friction factor (f_c), and Nusselt number (Nu_c) are calculated (using constricted parameters) and defined as

$$Re_c = \frac{\rho U d_c}{\mu} \quad (9) \qquad f_c = \frac{\Delta P d_c}{2\rho U^2 L} \quad (10) \qquad Nu_c = \frac{h d_c}{k_f} \quad (11) \qquad h = \frac{q}{T_w - T_f} \quad (12)$$

The pressure loss (ΔP) and convective heat transfer coefficient (h,) are calculated after the flow is fully developed in the channel.

The boundary conditions are set as follows:

The velocity inlet is applied at the channel inlet: $u = u_{in}$, $v = w = 0$, $T = T_{in}$. The top and bottom (rough) walls are under constant heat flux, q =190 W/m^2. The remaining walls (side; smooth) are assumed adiabatic, $\partial T/\partial x= \partial T/\partial y=\partial T/\partial z=0$. For the outlet, the pressure is set, P_{out} = 0. The computational domain is shown in Fig. 1(a). The above mentioned governing equations and boundary conditions are solved by the finite volume method with Fluent program [12]. The first-order upwind scheme for discretization of governing equations along with the SIMPLE algorithm for the velocity-pressure coupling is utilized to perform the numerical analysis.

4. Results and discussion

4.1. Grid independence and model validation

Grid independence tests are conducted using several different mesh sizes, and criterions for discrepancies of f_c are applied. ANSYS-Workbench is adopted to generate mesh and roughness models. The channel width of 12.7 mm is considered for the independence criteria. The discrepancies of f_c between 9, 13 and 15 million are 3% and 1%, respectively, as discussed in Table 1. Thus, results from grid sensitivity analysis show that mesh composed by tetra grid with 13 million is suitable for the present study.

Table 1
Grid independence verification

#	Grid # (10^6)	f_c	Difference (%)
1	4.3	0.28	-
2	6.5	0.273	2.5
3	9	0.261	4.4
4	13	0.252	3.4
5	15	0.249	1.1

Table 2
Case study for model validation.

Roughness	Re_c	r (μm)	H (μm)	Nu_c (Present)	Nu_c [8]
Sinusoidal	100	30	250	10.67	11.33
Sinusoidal	100	50	250	8.58	8.601

The present model is applied in the cases from a reference study [8], to validate the model. The details are listed in Table 2, and deviations are in the acceptable range.

4.2. Fluid flow and heat transfer

In the present study, micro- and mini-channels structured with surface roughness are studied for varying aspect ratios (0.015, 0.021, 0.038) and respective widths (W) are 12.7 mm, 8.95 mm and 5 mm. Fig. 2(a) shows that constricted friction factor (f_c) is higher for lower aspect ratio of channel (r and H are constant), i.e. f_c of α_c = 0.015 are 5% and 9% higher than that of α_c = 0.021 and α_c = 0.038, respectively at Re_c = 100. It means that increasing surface area of rough walls increases the frictional effect and hydraulic diameter also increases with the width. These higher frictional effects are also due to the additional effects of sharp bends and sudden change of flow direction after every roughness curve (Fig. 3).

Fig. 2(b) shows that lowering the α_c results in the increase of convective heat transfer (Nu_c). It also elaborates that increasing Re_c improves the Nu_c for all the α_c variations. It is clear from Fig. 2 that wetted perimeter variation is dominating as compared to hydraulic diameter. The larger wetted perimeters mean more convective heat transfer, as explained by Newton`s law of cooling. A smaller hydraulic diameter of rectangular micro-channel has a larger wetted perimeter and convection heat transfer area (between the working fluid and heat sink). This increases the heat transfer from the heat sink to the cooling medium and leads to higher cooling performance of heat sinks. Hence, Nu_c for α_c = 0.015 is 8% and 20% higher than that of α_c = 0.021 and α_c = 0.038, respectively. Fig. 3 elaborates another factor which shows that the flow velocities are higher in the case of higher α_c (Fig. 3(a)), but the flow disturbances are more in the channels with lower α_c. This phenomenon seems additive reason of higher convective heat transfer. Although, the boundary layer thickness of stagnant flow seems same in both the cases.

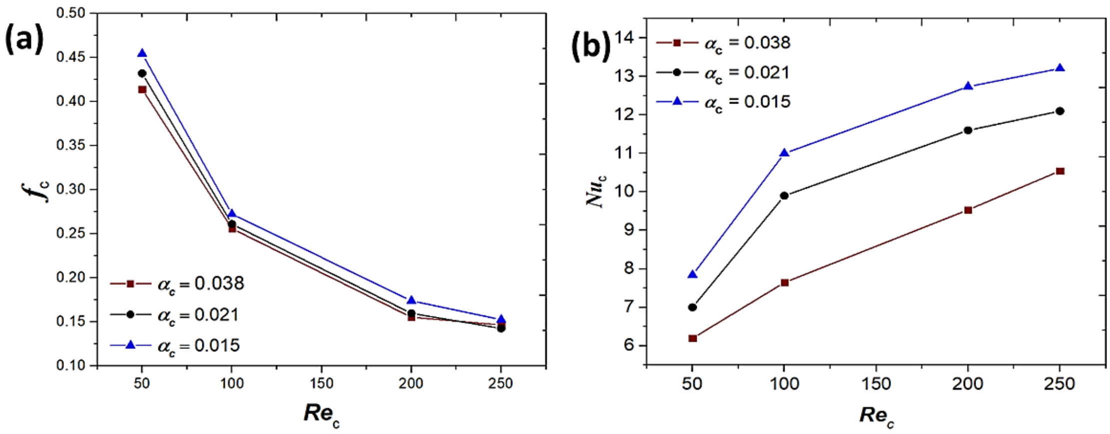

Fig. 2. Effect of channel aspect ratio on rough channels (a): f_c vs. Re_c; (b) Nu_c vs. Re_c.

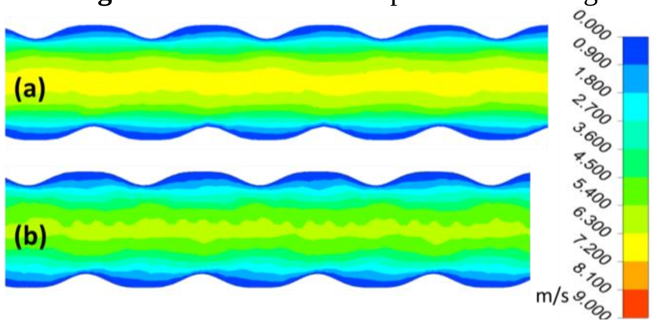

Fig. 3. Velocity contours of rough micro- and mini-channel heat sinks (Re_c = 100): (a) α_c = 0.038*;* (b) α_c = 0.021.

The results of the present study and correlations of smooth channels for Nusselt number are plotted in Fig. 4(a) to elaborate the comparison. The correlations are given below [1, 8],

$$Nu_s = 4.364 + \frac{0.0668(ReDPr/L)}{1+0.4(\frac{ReDPr}{L})^{2/3}} \tag{13}$$

$$Nu_{th} = 8.235(1 - 2.0421\alpha + 3.0853\alpha^2 - 2.4765\alpha^3 + 1.0578\alpha^4 - 0.1861\alpha^5) \tag{14}$$

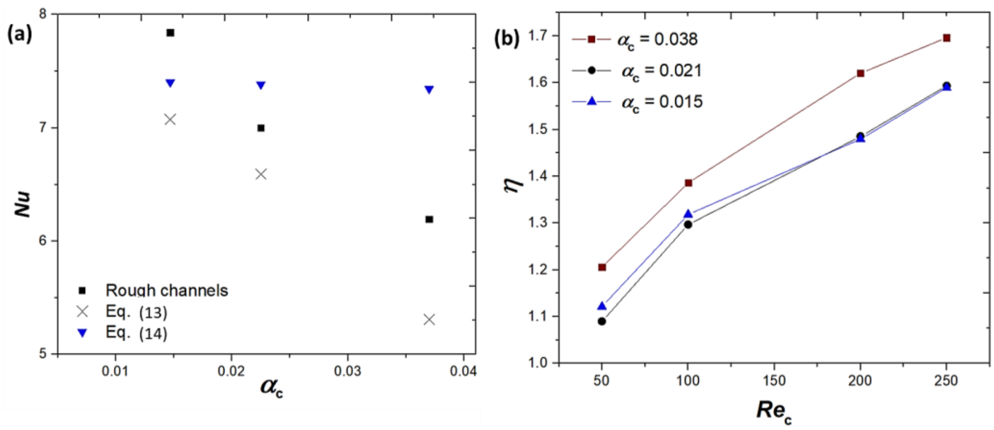

Fig. 4. (a) Comparison between present study and correlations, (Re_c = 100): Nu vs. α_c; (b) Effect of aspect ratio on rough channels: η vs. Re_c.

The calculated values (of Nu_c at Re_c = 100) are lower than the approximations of Eq. (14) (Shah and London) and higher than Eq. (13) (Grigull and Tartz). The trends of our simulations are close to the later one (Eq. (13)) because of the dependency on both Re_c and dimensional parameters of the channel. However, the higher heat exchange (Nu_c) of rough channels is the influence of structured sinusoidal roughness which leads to flow modifications and increased contact time with the heated wall. The α_c of these channels is very low as compared to size of the channels for which these correlations were developed and seems another reason of this discrepancy.

4.3. Thermohydraulic performance factor

The efficient heat sinks are the ones with maximum heat transfer and minimum frictional resistance. Thus, thermal performance factor η is gauged in terms of Nusselt number and frictional factor of both smooth and rough channels, given as

$$\eta = \frac{Nu_c/Nu_{th}}{({}^{f_c}/_{f_{th}})^{1/3}} \tag{15}$$

where f_{th} and Nu_{th} represent the corresponding theoretical friction factor and Nusselt number for smooth channels, respectively. Eqs. (14) and (16) are applied for the calculation of respective values of Nusselt number and friction factor of smooth channels [8].

$$f_{th} = \frac{24}{Re}\,(1 - 1.3553\alpha + 1.9467\alpha^2 - 1.7012\alpha^3 + 0.9564\alpha^4 - 0.2537\alpha^5) \tag{16}$$

Fig. 4(b) shows that the thermal performance factor is more than 1 for all the considered cases due to the positive impact of surface roughness and increasing with increasing Re_c. The highest values are observed for the channel of α_c = 0.038 due to the corresponding lower values of Nusselt number for smooth channels. The corresponding f_c is also lower for higher aspect ratio. The average rise of α_c = 0.038 at Re_c = 250 is almost 6% more than the other two variations (α_c = 0.021, α_c = 0.015).

5. Conclusion

Numerical simulations are carried out to study the effect of aspect ratio (channel widths) on micro- and mini-channels structured with sinusoidal roughness, and conclusions are as follows:

1. The maximum deviation of the f_c among the variations is not more than 10%.
2. The constricted Nusselt number (Nu_c) depends on both constricted aspect ratio (α_c) and Reynolds number (Re_c). The values are also higher than those predicted by the correlations due to the presence of roughness structures.
3. The increase in channel width (decreasing aspect ratio) results in the escalation of convective heat transfer.
4. The performance factor is increasing with increasing Re_c and at higher α_c. All the values are higher than 1 with a maximum value of 1.65 (at W = 5 mm and Re_c = 250).

6. References

[1] M Asadi G Xie B Sunden 2014 England. Int. J. Heat Mass Trans. 79 34-53.
[2] W Qu I Mudawar 2002 England. Int. J. Heat Mass Trans. 45 2549-2565.
[3] X Yuan Z Tao H Li Y Tian 2016 China. Chinese Journal of Aeronautics, 29 1575-1581.
[4] R Dey T Das S Chakraborty 2012 United States. Heat Trans. Eng. 33 425-446.
[5] H Wang Z Chen J Gao 2016 England. Appl. Therm. Eng. 107 870-879.
[6] S Shen J Xu J Zhou Y Chen 2006 England. Energy Conv. Manag. 47 1311-1325.
[7] V Dharaiya S Kandlikar 2013 England. Int. J. Heat Mass Trans. 57 190-201.
[8] M Kharati-Koopaee M Zare 2015 France. Int. J. Therm. Sci. 90 9-23.
[9] C Zhang Y Chen M Shi 2010 Switzerland. Chem. Eng. Proc. 49 1188-1192.
[10] I Ghani N Kamaruzaman N Sidik 2017 England. Int. J. Heat Mass Trans. 108 1969-1981.
[11] L Guo H Xu L Gong 2015 England. Appl. Therm. Eng. 84 399-408.
[12] A. Fluent, Theory Guide and User's Guide 2015 USA. Ansys Inc.

Acknowledgment

This work is supported in part by Scientific Research Foundation for the Returned Overseas Chinese Scholars, State Education Ministry (No.2012940) and the Fundamental Research Funds for the Central Universities (09MG25).